

Growing Excesses of New Scalars at the Electroweak Scale

Srimoy Bhattacharya^{1,*}, Guglielmo Coloretti^{2,3,†}, Andreas Crivellin^{2,3,‡}, Salah-Eddine Dahbi^{1,§}, Yaquan Fang^{4,5,¶}, Mukesh Kumar^{1,**} and Bruce Mellado^{1,6,††}

¹*School of Physics and Institute for Collider Particle Physics,*

University of the Witwatersrand, Johannesburg, Wits 2050, South Africa

²*Physik-Institut, Universität Zürich, Winterthurerstrasse 190, CH-8057 Zürich, Switzerland*

³*Paul Scherrer Institut, CH-5232 Villigen PSI, Switzerland*

⁴*Institute of High Energy Physics, 19B, Yuquan Road, Shijingshan District, Beijing, 100049, China*

⁵*University of Chinese Academy of Sciences (CAS),*

19A Yuquan Road, Shijingshan District, Beijing, 100049, China

⁶*Themba LABS, National Research Foundation, PO Box 722, Somerset West 7129, South Africa*

We combine searches for scalar resonances at the electroweak scale performed by the Large Hadron Collider experiments ATLAS and CMS where persisted excesses have been observed in recent years. Using both the side-bands of Standard Model Higgs analyses as well as dedicated beyond the Standard Model analyses, we find significant hints for new scalars at ≈ 95 GeV (S') and ≈ 152 GeV (S). The presence of a 95 GeV scalar is preferred over the Standard Model hypothesis by 3.8σ , while interpreting the 152 GeV excesses in a simplified model with resonant pair production of S via a new heavier scalar $H(270)$, a global significance of $\approx 5\sigma$ is obtained. While the production mechanism of the S' cannot yet be determined, data strongly favours the associated production of S , i.e. via the decay of a heavier boson $H(pp \rightarrow H \rightarrow SS^*)$. A possible alternative or complementary decay chain is $H \rightarrow SS'$, where $S \rightarrow WW^*$ (S') would be the source of the leptons (b -quarks) necessary to explain the multi-lepton anomalies found in Large Hadron Collider data.

I. INTRODUCTION

The Standard Model (SM) of particle physics is the mathematical description of the fundamental constituents of matter and their interactions at microscopic scales. It has been extensively and successfully tested [1–3], with the discovery of the Brout-Englert-Higgs boson (h) [4–7] in 2012 at the Large Hadron Collider (LHC) [8, 9] at CERN providing the last missing particle. Furthermore, measurements of the properties of this 125 GeV boson agree with the SM predictions [10–13].

Despite the overwhelming success of the SM, the existence of additional scalar bosons is not excluded as long as their role in electroweak symmetry breaking is sufficiently small. In fact, it is clear that the SM cannot be the ultimate fundamental theory of nature. It can neither account for the observed non-vanishing neutrino masses nor the existence of Dark Matter (DM) established at astrophysical scales. Moreover, the minimality of the SM Higgs sector, i.e. the presence of a single $SU(2)_L$ doublet scalar that simultaneously gives mass to the electroweak (EW) gauge bosons and all fermions, is not guaranteed by any symmetry or principle. In fact most New Physics (NP) models in the literature contain new scalars, such as $SU(2)_L$ singlets [14–16], doublets [17–21] and triplets [22–27]. Furthermore,

also models with an even more complex scalar sector, which are especially relevant for the excesses discussed in this work, such as the next-to-minimal two-Higgs-doublet model (N2HDM) [28–49], are frequently studied.

On the experimental side, LHC searches for new particles in general, and new scalars in particular, have not led to any discovery yet. However, the searches for additional Higgses have been mostly performed inclusively or with a limited number of topologies, such that significant regions of the phase-space remain unexplored. In particular, associated production received relatively little attention. In this context, in recent years the so-called “multi-lepton anomalies” emerged, which are constituted by several tensions in channels with multiple electrons and/or muons in the final states. These discrepancies are statistically significant and point towards associated production of EW scale new scalars [43, 50–54]. In particular, the multi-lepton anomalies are compatible with the direct production of a scalar H , with a mass of ≈ 270 GeV, that decays dominantly into a pair of lighter scalars, S . A sub-set of these anomalies contains non-resonant opposite sign, different flavour di-leptons final states (with and without the presence of b -quark jets), pointing towards the decay $S \rightarrow W^+W^- \rightarrow \ell^+\ell^-$, $\ell = e, \mu$ with $m_S = 150 \pm 5$ GeV [50].

In Ref. [55], we showed that the side-bands of the SM Higgs boson analyses of ATLAS [56–58] and CMS [59–62] in fact suggest the presence of a narrow scalar resonance with a mass of ≈ 151 GeV, produced in association with leptons and (b -)jets. Furthermore, several hints for the existence of a new neutral scalar S' with a mass of ≈ 95 GeV were presented by the CMS experiment [63–65]. While previous ATLAS analyses did not exclude this potential signal [66, 67], the latest result [68] shows

* bhattacharyasrimoy@gmail.com

† guglielmo.coloretti@physik.uzh.ch

‡ andreas.crivellin@psi.ch

§ salah-eddine.dahbi@cern.ch

¶ fangyq@ihep.ac.cn

** mukesh.kumar@cern.ch

†† bmellado@mail.cern.ch

a weaker-than-expected limit at this mass. Furthermore, an old LEP measurement suggests $e^+e^- \rightarrow Z^* \rightarrow S'Z$ with $Z \rightarrow b\bar{b}$ [69] and CMS finds a hint for resonant τ pair production at a similar mass [65].

In this article, we combine, for the first time, the hints for a 95 GeV scalar and extend and update the fit of Ref. [55] for the ≈ 151 GeV one by including the side-bands of the recently released analysis of associate production of the SM Higgs [70] as well as the WW channel analyzed in Ref. [71], in order to obtain combined evidence for new scalar resonances at the EW scale.

II. CHANNELS

A. Low mass range: S' (≈ 95 GeV)

$(S' \rightarrow b\bar{b}) + Z$: LEP reported an excess with a local significance of 2.3σ at ≈ 98 GeV in Higgsstrahlung, i.e. $e^+e^- \rightarrow ZS'$ with $S' \rightarrow b\bar{b}$ [69]. We will not include this excess directly in the combination, but rather use it to obtain a more narrow mass window of $93 \text{ GeV} < m_{S'} < 103 \text{ GeV}$ to reduce the look-elsewhere-effect (i.e. the trail factor).

$S' \rightarrow \gamma\gamma$: We use the p -value graph in Fig. 7 of the CMS analysis [64] and Figure 7 (a) of the ATLAS analysis [68].

$S' \rightarrow \tau\tau$: The relevant p -value graph is provided in the supplemental material of Ref. [65] and shows an excess with a local significance of 3.1σ . While ATLAS did not perform an explicit search for new scalars in this final state, Ref. [67] see no excess in the side-band of the SM Higgs boson analysis. We therefore treat this as a null result which reduces the significance of the CMS excess by a factor of $\sqrt{2}$, assuming that the ATLAS and CMS analyses have similar sensitivity.

$S' \rightarrow WW^*$: We use the combined transverse mass distributions of lower graphs of Fig. 2 in Ref. [72] (CMS) and the upper-left graph of Fig. 11 in Ref. [73] (ATLAS). The details of the combination and the simulation are described in Ref. [71] where an excess with a local significance of $\approx 2.6\sigma$ was found.

B. High mass range: S (≈ 152 GeV)

We utilise CMS and ATLAS studies of SM Higgses, which essentially encompass the search for other resonances in their side-bands. Depending on the channel, they range up to 180 GeV. However, because some analyses stop at 160 GeV. Since we want to avoid to be too close to the SM Higgs resonance, we will utilise the region between 140 GeV and 155-160 GeV, when appropriate.¹

The combination will be performed in two steps. The first combination includes data reported up until 2021.

$(S \rightarrow Z(\rightarrow \ell^+\ell^-)\gamma) + \ell$: The invariant mass of the $Z\gamma$ pair is used to reconstruct m_S and, in addition, the presence of an extra lepton (apart from the leptons produced by the Z decay) is required (Fig. 5 in Ref. [74]).

$(S \rightarrow \gamma\gamma) + E_{\text{miss}}^T$: m_S is reconstructed from the invariant mass of the photon pair and moderate additional missing energy of ≈ 100 GeV is required² (see Fig. 6 in Ref. [75] and Fig. 3 in Ref. [61]).

$(S \rightarrow b\bar{b}) + E_{\text{miss}}^T$: m_S is reconstructed from the invariant mass of the bottom quark pair and missing transverse energy is required (Fig. 14 (a) in Ref. [76]). Here, some overlap of this category and $t\bar{t}h$ production in the SM exists. However, the contamination of the former by the latter due to the production of E_{miss}^T from the decay of W s is quite minimal (approximately 1%).

$(S \rightarrow \gamma\gamma) + \mathbf{b\text{-jet}}$: In this channel, S decays to two photons and is produced in association with at least a b -jet. The experimental data is extracted from Fig. 2 (top-right) in Ref. [77] and Fig. 2 in Ref. [78].

$(S \rightarrow \gamma\gamma) + W, Z$: In this study, S decays to two photons and is produced in association with a weak gauge boson (W or Z). The relevant data is obtained from Fig. 15 (bottom-left) in Ref. [79] and Fig. 9 c) and d) in Ref. [56].

$S \rightarrow \gamma\gamma$ (inclusive): Also in the (quasi-)inclusive case, m_S is reconstructed from the invariant mass of the photon pair. However, vector boson fusion, as well as the presence of additional W and Z bosons and top quark-associated production are not included. Note that even though there is no veto on missing energy, the $S(\rightarrow \gamma\gamma) + E_{\text{miss}}^T$ channel only covers a small portion of phase space of the quasi-inclusive final search. Here we use Fig. 15 (top-left) of Ref. [79] and Fig. 9 a) of Ref. [56].

This determines a very narrow mass range of interest, thus avoiding further scanning, and removing look-elsewhere effects when including new data. In the second step, data from the following recent CMS and ATLAS analysis will be added to the first combination:

$(S \rightarrow \gamma\gamma) + \geq 4\mathbf{j}$: Here m_S corresponds to invariant mass of di-photon pair which is produced in association with at least 4 jets (Fig. 2 a) in Ref. [70]).

$(S \rightarrow WW^{(*)}) + E_{\text{miss}}^T$: The CMS and ATLAS analyses of the SM Higgs boson decaying to a pair of W bosons are recast and combined. Here we use the 0-jet category for which the dominant contribution from the simplified model described above arises from $H \rightarrow S(\rightarrow WW)S^*(\rightarrow E_{\text{miss}}^T)$. Other final states from associated production have very small jet veto survival probability. For ATLAS, we have used the data from Fig. 11 of Ref. [73] and for CMS the m_T distributions ($p_{T2} < 20$ GeV and $p_{T2} > 20$ GeV) of Fig. 1 of Ref. [72].

¹ Importantly, this mass range is suggested by, and compatible with, the multi-lepton anomalies.

² The range of missing energy is dictated by a predefined simplified model of $H \rightarrow SS^*$ and it is not determined by the experimental analysis.

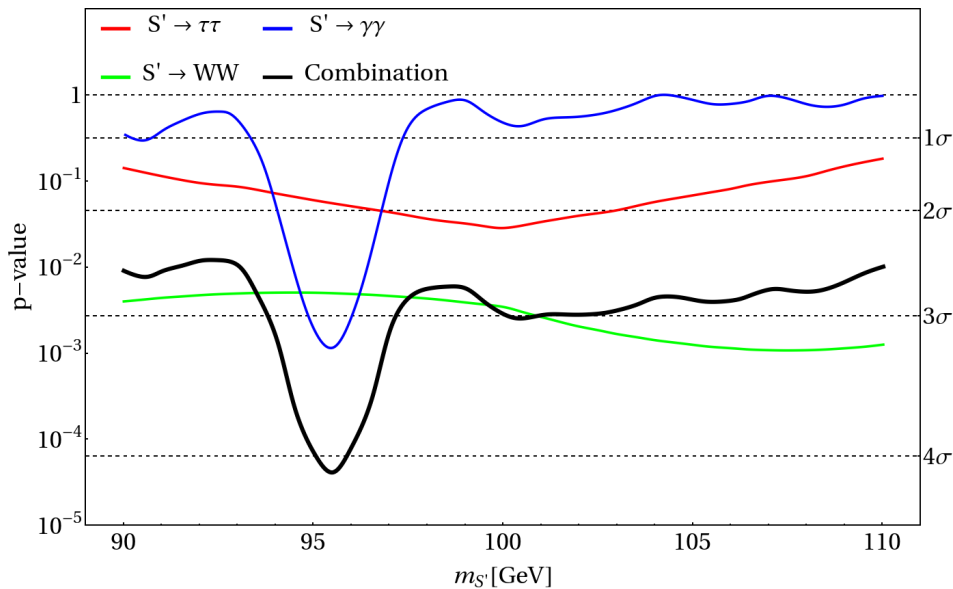


FIG. 1. The p -value as a function of the mass of S' for the low-mass channels (see main text for details).

$S(\rightarrow \gamma\gamma) + \geq 1\ell + b\text{-jet}$: S decays to two photons and is produced in association with at least one electron or muon (ℓ) and at least one tagged b -jet. The relevant experimental data are taken from Fig. 5 a) in Ref. [70].

$S(\rightarrow \gamma\gamma) + \gamma$: S , whose mass is obtained from the invariant mass of the leading and sub-leading photon, is produced in association with at least one additional photon moderate by $p_T \geq 25$ GeV (see Fig. 6 a in Ref. [70]).

$S \rightarrow e\mu$: Here we combine the data from ATLAS and CMS using the right-hand panel of Fig. 1 in Ref. [80] and Fig. 8 of Ref. [81]. However, since this signal is exotic and not easy to account for in a UV complete model [82, 83], we will show both the combinations with and without including this channel.

III. COMBINATIONS

A. Low mass range (95 GeV)

First, we combine the $\gamma\gamma$ results from ATLAS and CMS by assuming that both experiments have the same sensitivity to the signal see blue line in Fig. 1. We then add to this the $\tau\tau$ and $S \rightarrow WW^*$ signals, using Fisher's combined probability test [84] with three degrees of freedom (DOF):

$$\chi_{2n}^2 = -2 \sum_{i=1}^n \log(p_i), \quad (1)$$

where p_i is the p -value of each channel in the combination and χ_{2n}^2 represents the chi-squared distribution with $2n$ degrees of freedom, where n is the number of channels being combined.

The resulting χ^2 distribution is used to calculate the combined p -value shown in Fig. 1. The highest local significance of 4.1σ is obtained at $m_{S'} \approx 95$ GeV. Taking into account the LEP excess which narrows the mass range, the look-elsewhere effect, for a trial factor [85, 86] of $5/1.5 \approx 3.3$ (obtained from dividing half the mass range by the resolution of 1.5 GeV) [85], results in a global significance of 3.8σ .

B. High mass range (152 GeV)

The required main production mechanism here is clearly associated production. Therefore, we assume a simplified model with a scalar H , with a mass of 270 GeV and directly produced via gluon fusion (as motivated by the multi-lepton anomalies), which decays into two lighter ones where one of them is off-shell (SS^*).³ We assume S to be SM-like, i.e. to have the branching ratios of a hypothetical SM Higgs with the same mass [94–106].

In the first step, we assume an additional branching ratio to invisible final states. This means that the combination is thus performed with two DOFs. Considering only $\gamma\gamma$ and $Z\gamma$ channels for the on-shell S , we combine that data reported up to 2021.⁴ The blue line in Fig. 2 is obtained, corresponding to a maximal local significance

³ Refs. [43, 87] considered $H \rightarrow Sh$. While this has similar signatures than $H \rightarrow SS^*$, it leads to problems with SM Higgs signal strength measurements [88–93] if it is the dominant decay mode.

⁴ The observed yields of the $\gamma\gamma$ and $Z\gamma$ are consistent with those predicted by the simplified model. Other channels are considered in the second combination pass.

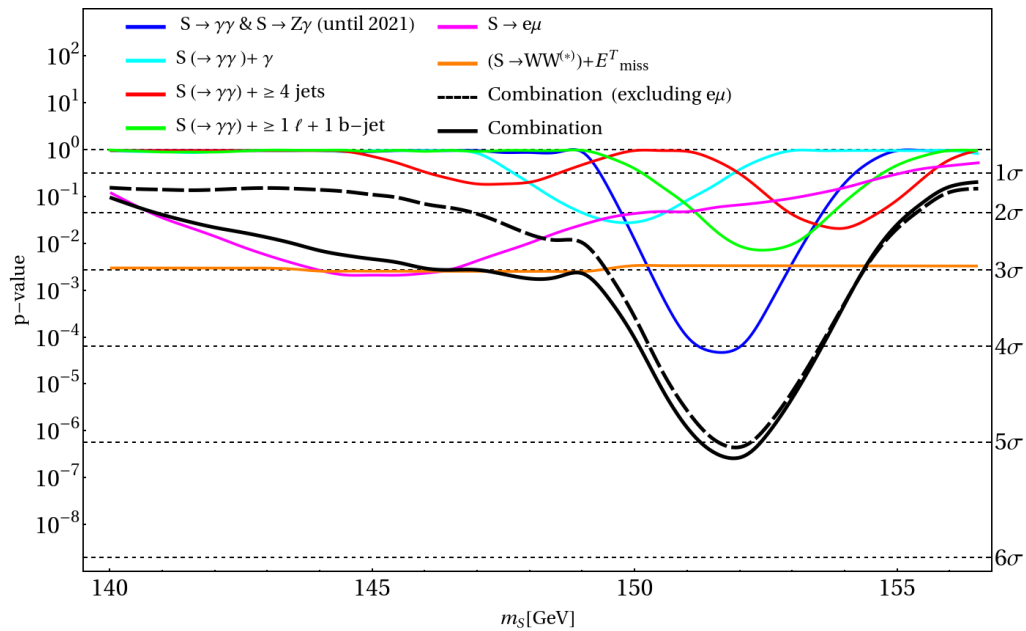


FIG. 2. The p -values of the individual high mass channels as well as their combination, both including and excluding the μe signal.

of 4.0σ at 152 GeV .⁵ The trials factor is computed taking into account the different signal resolutions and the mass range (140-155 GeV). This reduces the significance to 3.8σ . This result is combined with the results of the second combination for 152 GeV .

In order to verify the consistency between the observed signal yields of the data released after 2021 within this simplified model, we simulated the processes, $pp \rightarrow H \rightarrow SS^*$, where S decays to $S \rightarrow \gamma\gamma(Z\gamma)$ and S^* decays to $b\bar{b}$, $\tau^+\tau^-$, WW^* and missing energy. Again, we assumed that the ratios of the branching fractions of $b\bar{b}$ vs $\tau^+\tau^-$ and WW^* are SM-like. Afterwards, we applied the event selection criteria detailed in Ref. [70] to extract the signal efficiency of $S(\rightarrow \gamma\gamma) + \geq 4$ jets. The resulting expected yields from the simulation are found to be in agreement within 1σ with the observed yields from ATLAS.

A similar procedure is followed to analyze the cross-section for $S(\rightarrow WW^{(*)}) + E_{\text{miss}}^T$. The ratio of the extracted cross-sections of $S(\rightarrow \gamma\gamma) + E_{\text{miss}}^T$ to that of $S(\rightarrow WW^{(*)}) + E_{\text{miss}}^T$ is also consistent with the prediction of the simplified model. However, for purely SM-like branching ratios, the simplified model predicts an excess in $S \rightarrow ZZ^* \rightarrow 4\ell$, which is not observed. As such, the significance of the $S(\rightarrow WW^{(*)}) + E_{\text{miss}}^T$ is included in the combination with an additional DOF.

Because $(S \rightarrow \gamma\gamma) \geq 1\ell + b\text{-jet}$ and $(S \rightarrow \gamma\gamma) + \gamma$ are not predicted by the simplified model, they are added

using two additional DOF. The invariant mass spectra of the channels being combined are fitted with the sum of background and signal functions described in Eq. (A1) and Eq. (A2). The parameterization of each function takes into account the signal resolution of the channel, while the background corresponds to the SM hypothesis. Figure 2 shows the local p -value for the considered channels separately, where the significance for $(S \rightarrow \gamma\gamma) + \gamma$, $(S \rightarrow \gamma\gamma) + \geq 4$ jets and $(S \rightarrow \gamma\gamma) + \geq \ell + b\text{-jet}$ are calculated individually using the formula A3 with the weighted signal efficiency ϵ is equal to one.

We proceed similarly with the $S \rightarrow e\mu$ channel, which is not present in the simplified model. The combined results from ATLAS and CMS of $S \rightarrow e\mu$ channel are detailed in Appendix IV. Finally, all channels are combined using Fisher's combined probability Eq. 1 with five DOFs. Figure 2 displays the results, where a global significance of 5.0σ is found for $m_S = 152\text{ GeV}$. Since the $S \rightarrow e\mu$ signal is exotic, we also show the combination without this channel, leading to a global significance of 4.9σ .

IV. CONCLUSIONS

The multi-lepton anomalies signify the current statistically most significant deviation of LHC data from the SM predictions. They can be consistently explained by assuming a simplified model in which a heavy scalar H decays into two lighter scalars S with EW scale masses. Assuming a sizable decay width for $S \rightarrow W^+W^- \rightarrow \ell^+\ell^-$, $\ell = e, \mu$, the mass of the scalar was determined to be $m_S = 150 \pm 5\text{ GeV}$.

⁵ The largest local significance for this first combination is 4.1σ at 151.5 GeV . However, the largest significance in the global combination is obtained for 152 GeV . As such, the significance is reported for this mass.

Motivated by these anomalies and their possible explanations, we searched for narrow resonances in the side-bands of SM Higgs analysis and found a hint for a ≈ 151 GeV scalar [55]. In this article, we added to this combination the recent ATLAS and CMS analyses released after 2021 and found that the significance is further strengthened: assuming a simplified model with 5 DOF, we found $\approx 5\sigma$ for $m_S \approx 152$ GeV.

Furthermore, we combined the hints for the presence of a ≈ 95 GeV scalar S' , finding a preference of 3.8σ over the Standard Model hypothesis. This opens the possibility of a decay chain $H \rightarrow SS'$ explaining the multi-lepton anomalies. In this case, the decay of the S would be the source of leptons, while S' would be the origin of b -quarks. Finally, the absence of a $S \rightarrow ZZ^* \rightarrow 4\ell$ signal suggests that S could be the neutral component of an $SU(2)$ triplet [107–119], as motivated by average [120] of the W mass measurement [121–124].

ACKNOWLEDGMENTS

The work of A.C. is supported by a professorship grant from the Swiss National Science Foundation (No. PP00P21.76884). B.M. gratefully acknowledges the South African Department of Science and Innovation through the SA-CERN program, the National Research Foundation, and the Research Office of the University of the Witwatersrand for various forms of support.

Appendix A: Details of the analysis

1. $S \rightarrow \gamma\gamma$

As outlined in the introduction, we use CMS and ATLAS analyses to search for new scalars in the mass range between 90 GeV and 110 GeV as well as between 140 GeV and 155 GeV. For the side-band searches, for each category, we model the background via

$$f(m; b, \{a\}) = (1 - m)^b (m)^{a_0 + a_1 \log(m)}, \quad (\text{A1})$$

where $a_{0,1}$ and b are free parameters (different for each category) and m is the invariant mass of the distribution, e.g. the di-photon mass. The choice of the functional form to model the background is not important for our study, as shown in Ref. [55] to which the reader is referred to for more technical details.

We add to the background parametrized by Eq. (A1) a double-sided-crystal-ball function:

$$N \cdot \begin{cases} e^{-t^2/2} & \text{if } -\alpha_{\text{Low}} \leq t \leq \alpha_{\text{High}} \\ \frac{e^{-0.5\alpha_{\text{Low}}^2}}{\left[\frac{\alpha_{\text{Low}}}{\alpha_{\text{Low}}} \left(\frac{n_{\text{Low}}}{\alpha_{\text{Low}}} - \alpha_{\text{Low}} - t\right)\right]^{n_{\text{Low}}}} & \text{if } t < -\alpha_{\text{Low}} \\ \frac{e^{-0.5\alpha_{\text{High}}^2}}{\left[\frac{\alpha_{\text{High}}}{\alpha_{\text{High}}} \left(\frac{n_{\text{High}}}{\alpha_{\text{High}}} - \alpha_{\text{High}} + t\right)\right]^{n_{\text{High}}}} & \text{if } t > \alpha_{\text{High}}. \end{cases} \quad (\text{A2})$$

Here N is a normalization parameter, $t = (m - m_S)/\sigma_{CB}$ where σ_{CB} is the width of the Gaussian part of the function, m is the invariant mass of the distribution and m_S the mass of the new scalar.

2. $S \rightarrow WW$

We have simulated the process $pp \rightarrow H \rightarrow SS^*, S \rightarrow W^+W^{-(*)} \rightarrow \ell^+\ell^-\nu\bar{\nu}$ and S^* going to missing energy. Note that this is dominant compared to $S^* \rightarrow WW$ and S going to missing energy if the mass of the invisible particle is small. To validate and improve our fast simulation we simulated the SM Higgs boson signal, i.e. $gg \rightarrow h \rightarrow WW^{(*)} \rightarrow \ell^+\ell^-\nu\bar{\nu}$ and compared to the ATLAS one for the SM Higgs boson signal given as a function of the transverse mass m_T in Fig. 11 in Ref. [73]. In addition, smearing etc. was applied to correct for our fast simulation as explained in Ref. [71].

3. Combination of ATLAS and CMS data of the $S \rightarrow e\mu$ channel

The combination of ATLAS [80] and CMS [81] data are obtained from a simultaneous fit to the invariant mass of the electron–muon pair, in the mass range between 140 GeV and 157 GeV. The backgrounds in both ATLAS and CMS are parameterized using functional form in Eq. (A1) with different normalization factor to take in the account the difference in background contamination from each experiment. Afterward, we scanned the invariant mass spectrum of ATLAS and CMS simultaneously by adding a double-sided-crystal-ball function described in Eq. (A2), the parameter N of the added DSCB functions is considered as a common and free parameter, while the remaining parameters are fixed to the values extracted from the signal fit to Higgs-like scalar decaying to one electron and one muon in ATLAS and CMS detectors. Figure IV shows the combination of ATLAS and CMS data in the $S \rightarrow e\mu$ decay channel, where the individual significance is estimated using the median significance formula [86]

$$S = \sqrt{2} \sqrt{(\epsilon \cdot S + B) \log(1 + \epsilon \cdot S/B) - \epsilon \cdot S}. \quad (\text{A3})$$

Here, B and S are the continuum background and signal yields respectively, which are extracted from the simultaneous fit. While, the weighted signal efficiencies ϵ are found to be 55% and 45%, accordingly with the individual efficiency of the $S \rightarrow e\mu$ channel in the ATLAS and CMS analyses, respectively. Finally, the combined significance is calculated by summing the two individual significance in quadrature. After the combination, the ATLAS significance of 3.8σ at $m_S \approx 146$ GeV is reduced to 3.1σ by included the CMS result. Note that a significance of $\approx 2\sigma$ around $m_S = 151$ GeV is found.

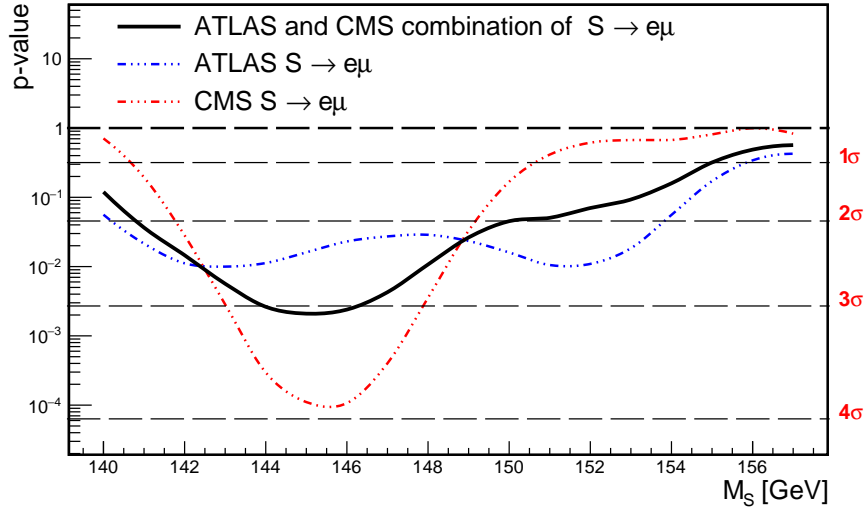


FIG. 3. Individual and combined p -values for $S' \rightarrow e\mu$ as a function of the mass.

-
- [1] R. L. Workman et al. (Particle Data Group), *PTEP* **2022**, 083C01 (2022).
- [2] Y. S. Amhis et al. (Heavy Flavor Averaging Group, HFLAV), *Phys. Rev. D* **107**, 052008 (2023), [arXiv:2206.07501 \[hep-ex\]](#).
- [3] S. Schael et al. (ALEPH, DELPHI, L3, OPAL, SLD, LEP Electroweak Working Group, SLD Electroweak Group, SLD Heavy Flavour Group), *Phys. Rept.* **427**, 257 (2006), [arXiv:hep-ex/0509008](#).
- [4] P. W. Higgs, *Phys. Lett.* **12**, 132 (1964).
- [5] F. Englert and R. Brout, *Phys. Rev. Lett.* **13**, 321 (1964).
- [6] P. W. Higgs, *Phys. Rev. Lett.* **13**, 508 (1964).
- [7] G. S. Guralnik, C. R. Hagen, and T. W. B. Kibble, *Phys. Rev. Lett.* **13**, 585 (1964).
- [8] G. Aad et al. (ATLAS), *Phys. Lett. B* **716**, 1 (2012), [arXiv:1207.7214 \[hep-ex\]](#).
- [9] S. Chatrchyan et al. (CMS), *Phys. Lett. B* **716**, 30 (2012), [arXiv:1207.7235 \[hep-ex\]](#).
- [10] S. Chatrchyan et al. (CMS), *Phys. Rev. Lett.* **110**, 081803 (2013), [arXiv:1212.6639 \[hep-ex\]](#).
- [11] G. Aad et al. (ATLAS), *Phys. Lett. B* **726**, 120 (2013), [arXiv:1307.1432 \[hep-ex\]](#).
- [12] J. M. Langford (ATLAS, CMS), *PoS LHCP2020*, 136 (2021).
- [13] “ATLAS Collaboration, “Combined measurements of Higgs boson production and decay using up to 139 fb⁻¹ of proton-proton collision data at $\sqrt{s} = 13$ TeV collected with the ATLAS experiment”, ATLAS-CONF-2021-053,” (2021).
- [14] V. Silveira and A. Zee, *Phys. Lett. B* **161**, 136 (1985).
- [15] M. Pietroni, *Nucl. Phys. B* **402**, 27 (1993), [arXiv:hep-ph/9207227](#).
- [16] J. McDonald, *Phys. Rev. D* **50**, 3637 (1994), [arXiv:hep-ph/0702143](#).
- [17] T. D. Lee, *Phys. Rev. D* **8**, 1226 (1973).
- [18] H. E. Haber and G. L. Kane, *Phys. Rept.* **117**, 75 (1985).
- [19] J. E. Kim, *Phys. Rept.* **150**, 1 (1987).
- [20] R. D. Peccei and H. R. Quinn, *Phys. Rev. Lett.* **38**, 1440 (1977).
- [21] N. Turok and J. Zadrozny, *Nucl. Phys. B* **358**, 471 (1991).
- [22] W. Konetschny and W. Kummer, *Phys. Lett. B* **70**, 433 (1977).
- [23] T. P. Cheng and L.-F. Li, *Phys. Rev. D* **22**, 2860 (1980).
- [24] G. Lazarides, Q. Shafi, and C. Wetterich, *Nucl. Phys. B* **181**, 287 (1981).
- [25] J. Schechter and J. W. F. Valle, *Phys. Rev. D* **22**, 2227 (1980).
- [26] M. Magg and C. Wetterich, *Phys. Lett. B* **94**, 61 (1980).
- [27] R. N. Mohapatra and G. Senjanovic, *Phys. Rev. D* **23**, 165 (1981).
- [28] X.-G. He, T. Li, X.-Q. Li, J. Tandean, and H.-C. Tsai, *Phys. Rev. D* **79**, 023521 (2009), [arXiv:0811.0658 \[hep-ph\]](#).
- [29] B. Grzadkowski and P. Osland, *Phys. Rev. D* **82**, 125026 (2010), [arXiv:0910.4068 \[hep-ph\]](#).
- [30] H. E. Logan, *Phys. Rev. D* **83**, 035022 (2011), [arXiv:1010.4214 \[hep-ph\]](#).
- [31] M. S. Boucenna and S. Profumo, *Phys. Rev. D* **84**, 055011 (2011), [arXiv:1106.3368 \[hep-ph\]](#).
- [32] X.-G. He, B. Ren, and J. Tandean, *Phys. Rev. D* **85**, 093019 (2012), [arXiv:1112.6364 \[hep-ph\]](#).
- [33] Y. Bai, V. Barger, L. L. Everett, and G. Shaughnessy, *Phys. Rev. D* **88**, 015008 (2013), [arXiv:1212.5604 \[hep-ph\]](#).
- [34] X.-G. He and J. Tandean, *Phys. Rev. D* **88**, 013020 (2013), [arXiv:1304.6058 \[hep-ph\]](#).
- [35] Y. Cai and T. Li, *Phys. Rev. D* **88**, 115004 (2013), [arXiv:1308.5346 \[hep-ph\]](#).
- [36] C.-Y. Chen, M. Freid, and M. Sher, *Phys. Rev. D* **89**, 075009 (2014), [arXiv:1312.3949 \[hep-ph\]](#).

- [37] J. Guo and Z. Kang, *Nucl. Phys. B* **898**, 415 (2015), [arXiv:1401.5609 \[hep-ph\]](#).
- [38] L. Wang and X.-F. Han, *Phys. Lett. B* **739**, 416 (2014), [arXiv:1406.3598 \[hep-ph\]](#).
- [39] A. Drozd, B. Grzadkowski, J. F. Gunion, and Y. Jiang, *JHEP* **11**, 105 (2014), [arXiv:1408.2106 \[hep-ph\]](#).
- [40] P. Ko, Y. Omura, and C. Yu, *JHEP* **11**, 054 (2014), [arXiv:1405.2138 \[hep-ph\]](#).
- [41] R. Campbell, S. Godfrey, H. E. Logan, A. D. Peterson, and A. Poulin, *Phys. Rev. D* **92**, 055031 (2015), [Erratum: *Phys.Rev.D* 101, 039905 (2020)], [arXiv:1505.01793 \[hep-ph\]](#).
- [42] A. Drozd, B. Grzadkowski, J. F. Gunion, and Y. Jiang, *JCAP* **10**, 040 (2016), [arXiv:1510.07053 \[hep-ph\]](#).
- [43] S. von Buddenbrock, N. Chakrabarty, A. S. Cornell, D. Kar, M. Kumar, T. Mandal, B. Mellado, B. Mukhopadhyaya, R. G. Reed, and X. Ruan, *Eur. Phys. J. C* **76**, 580 (2016), [arXiv:1606.01674 \[hep-ph\]](#).
- [44] A. Arhrib, R. Benbrik, M. El Kacimi, L. Rahili, and S. Semlali, *Eur. Phys. J. C* **80**, 13 (2020), [arXiv:1811.12431 \[hep-ph\]](#).
- [45] I. Engeln, P. Ferreira, M. M. Mühlleitner, R. Santos, and J. Wittbrodt, *JHEP* **08**, 085 (2020), [arXiv:2004.05382 \[hep-ph\]](#).
- [46] D. Azevedo, P. Gabriel, M. Muhleitner, K. Sakurai, and R. Santos, *JHEP* **10**, 044 (2021), [arXiv:2104.03184 \[hep-ph\]](#).
- [47] T. Biekötter, S. Heinemeyer, and G. Weiglein, *Eur. Phys. J. C* **83**, 450 (2023), [arXiv:2204.05975 \[hep-ph\]](#).
- [48] S. Banik, A. Crivellin, S. Iguro, and T. Kitahara, (2023), [arXiv:2303.11351 \[hep-ph\]](#).
- [49] T. Biekötter, S. Heinemeyer, and G. Weiglein, (2023), [arXiv:2306.03889 \[hep-ph\]](#).
- [50] S. von Buddenbrock, A. S. Cornell, A. Fadol, M. Kumar, B. Mellado, and X. Ruan, *J. Phys. G* **45**, 115003 (2018), [arXiv:1711.07874 \[hep-ph\]](#).
- [51] S. Buddenbrock, A. S. Cornell, Y. Fang, A. Fadol Mohammed, M. Kumar, B. Mellado, and K. G. Tomiwa, *JHEP* **10**, 157 (2019), [arXiv:1901.05300 \[hep-ph\]](#).
- [52] S. von Buddenbrock, R. Ruiz, and B. Mellado, *Phys. Lett. B* **811**, 135964 (2020), [arXiv:2009.00032 \[hep-ph\]](#).
- [53] Y. Hernandez, M. Kumar, A. S. Cornell, S.-E. Dahbi, Y. Fang, B. Lieberman, B. Mellado, K. Monnakgotla, X. Ruan, and S. Xin, *Eur. Phys. J. C* **81**, 365 (2021), [arXiv:1912.00699 \[hep-ph\]](#).
- [54] O. Fischer et al., *Eur. Phys. J. C* **82**, 665 (2022), [arXiv:2109.06065 \[hep-ph\]](#).
- [55] A. Crivellin, Y. Fang, O. Fischer, A. Kumar, M. Kumar, E. Malwa, B. Mellado, N. Rapheeha, X. Ruan, and Q. Sha, (2021), [arXiv:2109.02650 \[hep-ph\]](#).
- [56] “ATLAS Collaboration, “Measurement of the properties of Higgs boson production at $\sqrt{s}=13$ TeV in the $H \rightarrow \gamma\gamma$ channel using 139 fb $^{-1}$ of pp collision data with the ATLAS experiment, ATLAS-CONF-2020-026,” (2020).
- [57] G. Aad et al. (ATLAS), *Phys. Rev. Lett.* **125**, 061802 (2020), [arXiv:2004.04545 \[hep-ex\]](#).
- [58] G. Aad et al. (ATLAS), *JHEP* **10**, 013 (2021), [arXiv:2104.13240 \[hep-ex\]](#).
- [59] A. M. Sirunyan et al. (CMS), *JHEP* **07**, 027 (2021), [arXiv:2103.06956 \[hep-ex\]](#).
- [60] A. M. Sirunyan et al. (CMS), *Phys. Rev. Lett.* **125**, 061801 (2020), [arXiv:2003.10866 \[hep-ex\]](#).
- [61] A. M. Sirunyan et al. (CMS), *JHEP* **09**, 046 (2018), [arXiv:1806.04771 \[hep-ex\]](#).
- [62] A. M. Sirunyan et al. (CMS), *JHEP* **11**, 152 (2018), [arXiv:1806.05996 \[hep-ex\]](#).
- [63] A. M. Sirunyan et al. (CMS), *Phys. Lett. B* **793**, 320 (2019), [arXiv:1811.08459 \[hep-ex\]](#).
- [64] “CMS Collaboration, “Search for a standard model-like Higgs boson in the mass range between 70 and 110 GeV in the diphoton final state in proton-proton collisions at $\sqrt{s} = 13$ TeV”, CMS-PAS-HIG-20-002,” (2023).
- [65] “CMS Collaboration, “Searches for additional Higgs bosons and for vector leptoquarks in $\tau\tau$ final states in proton-proton collisions at $\sqrt{s} = 13$ TeV”, CMS-HIG-21-001, CERN-EP-2022-137,” (2022), [arXiv:2208.02717 \[hep-ex\]](#).
- [66] “ATLAS Collaboration, “Search for resonances in the 65 to 110 GeV diphoton invariant mass range using 80 fb $^{-1}$ of pp collisions collected at $\sqrt{s} = 13$ TeV with the ATLAS detector”, ATLAS-CONF-2018-025,” (2018).
- [67] G. Aad et al. (ATLAS), *JHEP* **08**, 175 (2022), [arXiv:2201.08269 \[hep-ex\]](#).
- [68] “ATLAS Collaboration, “Search for diphoton resonances in the 66 to 110 GeV mass range using 140 fb $^{-1}$ of 13 TeV pp collisions collected with the ATLAS detector”, ATLAS-CONF-2023-035,” (2023).
- [69] R. Barate et al. (LEP Working Group for Higgs boson searches, ALEPH, DELPHI, L3, OPAL), *Phys. Lett. B* **565**, 61 (2003), [arXiv:hep-ex/0306033](#).
- [70] “ATLAS Collaboration, “Model-independent search for the presence of new physics in events including $H \rightarrow \gamma\gamma$ with $\sqrt{s} = 13$ TeV pp data recorded by the ATLAS detector at the LHC,” (2023), [arXiv:2301.10486 \[hep-ex\]](#).
- [71] G. Coloretti, A. Crivellin, S. Bhattacharya, and B. Mellado, (2023), [arXiv:2302.07276 \[hep-ph\]](#).
- [72] “CMS Collaboration, “Measurements of the Higgs boson production cross section and couplings in the W boson pair decay channel in proton-proton collisions at $\sqrt{s} = 13$ TeV,” (2022), [arXiv:2206.09466 \[hep-ex\]](#).
- [73] “ATLAS Collaboration, “Measurements of Higgs boson production by gluon-gluon fusion and vector-boson fusion using $H \rightarrow WW^* \rightarrow e\nu\mu\nu$ decays in pp collisions at $\sqrt{s} = 13$ TeV with the ATLAS detector,” (2022), [arXiv:2207.00338 \[hep-ex\]](#).
- [74] A. M. Sirunyan et al. (CMS), *JHEP* **11**, 152 (2018), [arXiv:1806.05996 \[hep-ex\]](#).
- [75] G. Aad et al. (ATLAS), *JHEP* **10**, 013 (2021), [arXiv:2104.13240 \[hep-ex\]](#).
- [76] G. Aad et al. (ATLAS), *Eur. Phys. J. C* **81**, 178 (2021), [arXiv:2007.02873 \[hep-ex\]](#).
- [77] G. Aad et al. (ATLAS), *Phys. Rev. Lett.* **125**, 061802 (2020), [arXiv:2004.04545 \[hep-ex\]](#).
- [78] A. M. Sirunyan et al. (CMS), *Phys. Rev. Lett.* **125**, 061801 (2020), [arXiv:2003.10866 \[hep-ex\]](#).
- [79] A. M. Sirunyan et al. (CMS), *JHEP* **07**, 027 (2021), [arXiv:2103.06956 \[hep-ex\]](#).
- [80] G. Aad et al. (ATLAS), *Phys. Lett. B* **801**, 135148 (2020), [arXiv:1909.10235 \[hep-ex\]](#).
- [81] “CMS Collaboration, “Search for the lepton flavor violating decay of a Higgs boson in the $e\mu$ final state in proton-proton collisions at $\sqrt{s} = 13$ TeV”, CMS-PAS-HIG-22-002,” (2023).
- [82] R. Primulando, J. Julio, N. Srimanobhas, and P. Uttayarat, (2023), [arXiv:2304.13757 \[hep-ph\]](#).

- [83] Y. Afik, P. S. B. Dev, and A. Thapa, (2023), [arXiv:2305.19314 \[hep-ph\]](#).
- [84] R. Fisher, Statistical Methods for Research Workers (Oliver and Boyd, Edinburgh, Scotland, 1925).
- [85] E. Gross and O. Vitells, *Eur. Phys. J. C* **70**, 525 (2010), [arXiv:1005.1891 \[physics.data-an\]](#).
- [86] R. J. Barlow, *CERN Yellow Rep. School Proc.* **5**, 149 (2020), [arXiv:1905.12362 \[physics.data-an\]](#).
- [87] S. von Buddenbrock, A. S. Cornell, E. D. R. Iarilala, M. Kumar, B. Mellado, X. Ruan, and E. M. Shrif, *J. Phys. G* **46**, 115001 (2019), [arXiv:1809.06344 \[hep-ph\]](#).
- [88] V. Khachatryan et al. (CMS), *Phys. Rev. D* **92**, 012004 (2015), [arXiv:1411.3441 \[hep-ex\]](#).
- [89] G. Aad et al. (ATLAS), *Eur. Phys. J. C* **75**, 476 (2015), [Erratum: *Eur.Phys.J.C* 76, 152 (2016)], [arXiv:1506.05669 \[hep-ex\]](#).
- [90] V. Khachatryan et al. (CMS), *Eur. Phys. J. C* **75**, 212 (2015), [arXiv:1412.8662 \[hep-ex\]](#).
- [91] G. Aad et al. (ATLAS), *Eur. Phys. J. C* **76**, 6 (2016), [arXiv:1507.04548 \[hep-ex\]](#).
- [92] A. Tumasyan et al. (CMS), *Nature* **607**, 60 (2022), [arXiv:2207.00043 \[hep-ex\]](#).
- [93] *Nature* **607**, 52 (2022), [Erratum: *Nature* 612, E24 (2022)], [arXiv:2207.00092 \[hep-ex\]](#).
- [94] D. de Florian et al. (LHC Higgs Cross Section Working Group), **2/2017** (2016), [10.23731/CYRM-2017-002](#), [arXiv:1610.07922 \[hep-ph\]](#).
- [95] E. Braaten and J. P. Leveille, *Phys. Rev. D* **22**, 715 (1980).
- [96] N. Sakai, *Phys. Rev. D* **22**, 2220 (1980).
- [97] T. Inami and T. Kubota, *Nucl. Phys. B* **179**, 171 (1981).
- [98] S. G. Gorishnii, A. L. Kataev, and S. A. Larin, *Sov. J. Nucl. Phys.* **40**, 329 (1984).
- [99] S. G. Gorishnii, A. L. Kataev, S. A. Larin, and L. R. Surguladze, *Phys. Lett. B* **256**, 81 (1991).
- [100] S. G. Gorishnii, A. L. Kataev, S. A. Larin, and L. R. Surguladze, *Mod. Phys. Lett. A* **5**, 2703 (1990).
- [101] S. G. Gorishnii, A. L. Kataev, S. A. Larin, and L. R. Surguladze, *Phys. Rev. D* **43**, 1633 (1991).
- [102] A. Djouadi, P. Gambino, and B. A. Kniehl, *Nucl. Phys. B* **523**, 17 (1998), [arXiv:hep-ph/9712330](#).
- [103] G. Degrassi and F. Maltoni, *Nucl. Phys. B* **724**, 183 (2005), [arXiv:hep-ph/0504137](#).
- [104] G. Passarino, C. Sturm, and S. Uccirati, *Phys. Lett. B* **655**, 298 (2007), [arXiv:0707.1401 \[hep-ph\]](#).
- [105] S. Actis, G. Passarino, C. Sturm, and S. Uccirati, *Nucl. Phys. B* **811**, 182 (2009), [arXiv:0809.3667 \[hep-ph\]](#).
- [106] M. Spira, A. Djouadi, and P. M. Zerwas, *Phys. Lett. B* **276**, 350 (1992).
- [107] M. Chabab, M. C. Peyranère, and L. Rahili, *Eur. Phys. J. C* **78**, 873 (2018), [arXiv:1805.00286 \[hep-ph\]](#).
- [108] P. Fileviez Perez, H. H. Patel, and A. D. Plascencia, *Phys. Lett. B* **833**, 137371 (2022), [arXiv:2204.07144 \[hep-ph\]](#).
- [109] Y. Cheng, X.-G. He, F. Huang, J. Sun, and Z.-P. Xing, *Nucl. Phys. B* **989**, 116118 (2023), [arXiv:2208.06760 \[hep-ph\]](#).
- [110] T.-K. Chen, C.-W. Chiang, and K. Yagyu, *Phys. Rev. D* **106**, 055035 (2022), [arXiv:2204.12898 \[hep-ph\]](#).
- [111] T. G. Rizzo, *Phys. Rev. D* **106**, 035024 (2022), [arXiv:2206.09814 \[hep-ph\]](#).
- [112] W. Chao, M. Jin, H.-J. Li, and Y.-Q. Peng, (2022), [arXiv:2210.13233 \[hep-ph\]](#).
- [113] J.-W. Wang, X.-J. Bi, P.-F. Yin, and Z.-H. Yu, *Phys. Rev. D* **106**, 055001 (2022), [arXiv:2205.00783 \[hep-ph\]](#).
- [114] Y. Shimizu and S. Takeshita, (2023), [arXiv:2303.11070 \[hep-ph\]](#).
- [115] G. Lazarides, R. Maji, R. Roshan, and Q. Shafi, *Phys. Rev. D* **106**, 055009 (2022), [arXiv:2205.04824 \[hep-ph\]](#).
- [116] G. Senjanović and M. Zantedeschi, *Phys. Lett. B* **837**, 137653 (2023), [arXiv:2205.05022 \[hep-ph\]](#).
- [117] A. Crivellin, M. Kirk, and A. Thapa, (2023), [arXiv:2305.03081 \[hep-ph\]](#).
- [118] T.-K. Chen, C.-W. Chiang, and K. Yagyu, *JHEP* **06**, 069 (2023), [arXiv:2303.09294 \[hep-ph\]](#).
- [119] S. Ashanujjaman, S. Banik, G. Coloretti, A. Crivellin, B. Mellado, and A.-T. Mulaudzi, (2023), [arXiv:2306.15722 \[hep-ph\]](#).
- [120] J. de Blas, M. Pierini, L. Reina, and L. Silvestrini, *Phys. Rev. Lett.* **129**, 271801 (2022), [arXiv:2204.04204 \[hep-ph\]](#).
- [121] T. Aaltonen et al. (CDF), *Science* **376**, 170 (2022).
- [122] (2023).
- [123] R. Aaij et al. (LHCb), *JHEP* **01**, 036 (2022), [arXiv:2109.01113 \[hep-ex\]](#).
- [124] S. Schael et al. (ALEPH, DELPHI, L3, OPAL, LEP Electroweak), *Phys. Rept.* **532**, 119 (2013), [arXiv:1302.3415 \[hep-ex\]](#).